CORA Cork Open Research Archive
Cartlann Taighde Oscailte Chorcaí

Title	Graphene facilitates biomethane production from protein derived glycine in anaerobic digestion
Authors	Lin, Richen;Deng, Chen;Cheng, Jun;Xia, Ao;Lens, Piet N. L.;Jackson, Stephen A.;Dobson, Alan D. W.;Murphy, Jerry D.
Publication date	2018-11-22
Original Citation	Lin, R., Deng, C., Cheng, J., Xia, A., Lens, P. N. L., Jackson, S. A., Dobson, A. D. W. and Murphy, J. D. (2018) 'Graphene facilitates biomethane production from protein derived glycine in anaerobic digestion', iScience. 10, pp. 158-170. doi:10.1016/j.isci.2018.11.030
Type of publication	Article (peer-reviewed)
Link to publisher's version	10.1016/j.isci.2018.11.030
Rights	© 2018, the Authors. This is an open access article under the CC BY-NC-ND license (http://creativecommons.org/licenses/by-nc-nd/4.0/) - http://creativecommons.org/licenses/by-nc-nd/4.0/
Download date	2026-11-06 11:39:52
Item downloaded from	https://hdl.handle.net/10468/7195



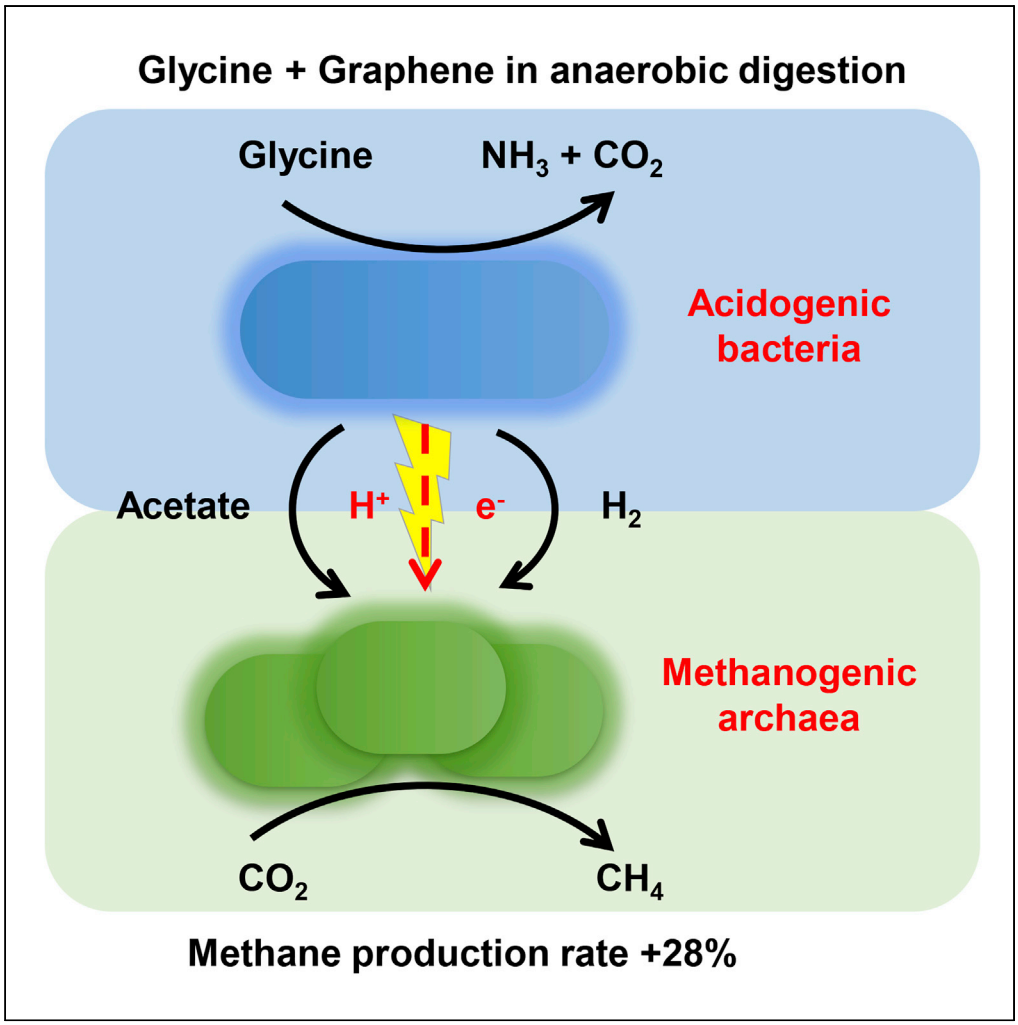
University College Cork, Ireland
Coláiste na hOllscoile Corcaigh

iScience

CellPress

Article

Graphene Facilitates Biomethane Production from Protein-Derived Glycine in Anaerobic Digestion



Richen Lin, Chen Deng, Jun Cheng, ..., Stephen A. Jackson, Alan D.W. Dobson, Jerry D. Murphy

richen.lin@ucc.ie

HIGHLIGHTS

Graphene led to an increase in peak bio-CH_4 production rate from glycine by 28%

Kinetic parameters had linear correlations with graphene addition (0.25–1.0 g/L)

Direct interspecies electron transfer (DIET) contributed to the improved performance

Lin et al., iScience *10*, 158–170
December 21, 2018 © 2018 The Author(s).
https://doi.org/10.1016/j.isci.2018.11.030

iScience

CellPress

Article

Graphene Facilitates Biomethane Production from Protein-Derived Glycine in Anaerobic Digestion

Richen Lin,[1,2,7,*] Chen Deng,[1,2] Jun Cheng,[3] Ao Xia,[4] Piet N.L. Lens,[5] Stephen A. Jackson,[1,6] Alan D.W. Dobson,[1,6] and Jerry D. Murphy[1,2]

SUMMARY

Interspecies electron transfer is a fundamental factor determining the efficiency of anaerobic digestion (AD), which involves syntrophy between fermentative bacteria and methanogens. Direct interspecies electron transfer (DIET) induced by conductive materials can optimize this process offering a significant improvement over indirect electron transfer. Herein, conductive graphene was applied in the AD of protein-derived glycine to establish DIET. The electron-producing reaction via DIET is thermodynamically more favorable and exhibits a more negative Gibbs free energy value (−60.0 kJ/mol) than indirect hydrogen transfer (−33.4 kJ/mol). The Gompertz model indicated that the kinetic parameters exhibited linear correlations with graphene addition from 0.25 to 1.0 g/L, leading to the highest increase in peak biomethane production rate of 28%. *Sedimentibacter* (7.8% in abundance) and archaea *Methanobacterium* (71.1%) and *Methanosarcina* (11.3%) might be responsible for DIET. This research can open up DIET to a range of protein-rich substrates, such as algae.

INTRODUCTION

The European Union (EU) has committed to achieving at least 20% renewable energy share of gross energy consumption by 2020, rising to at least 27% by 2030 (European Commission, 2016). Transport is the most difficult sector to decarbonize. This is reflected in the relatively low targets set by the EU. The target for advanced biofuels, including biogas not sourced from food crops (such as wastes and algae), has been set at a minimum share of 3.6% of the total fuel consumption by 2030; the target for 2021 is just 0.5% (European Commission, 2016). Anaerobic digestion (AD) is a well-established technology for waste management and production of renewable energy in which wet organic materials are broken down and converted into biogas by a variety of microorganisms, primarily including acidogenic bacteria and methanogenic archaea. In addition to biogas production from AD, other value-added chemicals (such as medium-chain carboxylic acids), can also be produced through the anaerobic process (Xu et al., 2018). In recent years, a rapid growth in newly installed biomethane plants has been observed. The European Biogas Association reported that the biomethane plants in the EU in 2015 were capable of producing 1,230 M Nm^3 of biomethane (European Biogas Association, 2016). This is readily available as transport fuel in natural gas vehicles. The market for biomethane, especially in the transport sector, will be driven by policy and renewable targets. Beyond the EU, the International Energy Agency (IEA) has suggested that biomethane for transport should rise to 3.74 EJ by 2040 from a base of 45.5 TJ in 2015 (IEA Energy Technology Perspectives, 2017; European Biogas Association, 2016). For this remarkable rise in biomethane production to be achieved using the world's finite resources, AD efficiency must be optimized, and challenging novel abundant feedstocks (such as algae) must be assessed for biomethane production.

Many studies and reviews are available that detail technology advantages and disadvantages, diverse microbial pathways, and challenges involved in AD (FitzGerald et al., 2015; Xia et al., 2016; Batstone and Virdis, 2014; Rotaru et al., 2014b). Studies have shown that digestion of complex feedstocks is not entirely efficient. Protein-rich feedstocks (such as algae) may be difficult to handle in AD owing to the presence of unfavorable protein components and unbalanced carbon to nitrogen ratios, which together may lead to process instability, sub-optimal digestion, and, ultimately, failure. If the resource of biomethane is projected to increase as suggested by the IEA, then difficult feedstocks such as algae with a huge biomethane resource must be digested as efficiently as possible. Thus far, the efficiency of digestion of protein-rich feedstocks reported varies from 20% to 70% (Mei et al., 2016). In general, for slowly biodegradable

[1]MaREI Centre, Environmental Research Institute, University College Cork, Cork, Ireland

[2]School of Engineering, University College Cork, Cork, Ireland

[3]State Key Laboratory of Clean Energy Utilization, Zhejiang University, Hangzhou 310027, China

[4]Key Laboratory of Low-grade Energy Utilization Technologies and Systems, Chongqing University, Ministry of Education, Chongqing 400044, China

[5]National University of Ireland Galway, University Road, Galway, Ireland

[6]School of Microbiology, University College Cork, Cork, Ireland

[7]Lead Contact

*Correspondence: richen.lin@ucc.ie

https://doi.org/10.1016/j.isci.2018.11.030

 © 2018 The Author(s).
This is an open access article under the CC BY-NC-ND license (http://creativecommons.org/licenses/by-nc-nd/4.0/).

substrates (such as polysaccharides and proteins), hydrolysis is the rate-limiting step (Ariunbaatar et al., 2014). However, when the substrates are easily degradable organics, such as monosaccharides or amino acids, the digestion process is limited by methanogenesis rather than by hydrolysis. Based on the current understanding of the microbiology of AD, the inefficiency and instability of digestion can be fundamentally optimized through the microbial interspecies electron transfer between acidogenic bacteria and methanogenic archaea.

The predominant understanding of interspecies electron transfer in AD is based on mediated interspecies electron transfer (MIET), in which hydrogen gas produced by acidogenic bacteria diffuses to hydrogenotrophic methanogens. However, from a thermodynamic perspective, the success of MIET is strongly restricted to the metabolite concentration, especially hydrogen. If the hydrogen partial pressure is high acidogenic bacteria are inhibited, whereas hydrogenotrophic methanogenic archaea by consuming hydrogen facilitate enhanced performance of the acidogenic bacteria. As an alternative, direct interspecies electron transfer (DIET) via biological pili or shuttle molecules is recognized as an improvement of this process, replacing hydrogen as the electron carrier between bacteria and archaea. Conductive materials might act as an effective electron conduit among microorganisms. Growing evidence suggests that the addition of conductive materials, such as ferroferric oxide, biochar, carbon nanotube, and graphene, can improve AD performance in terms of reducing lag phase time, increasing methane production rate, and resisting inhibitory conditions (Zhao et al., 2017; Lee et al., 2016; Yan et al., 2017; Yin et al., 2018).

Zhao et al. (Zhao et al., 2017) demonstrated that anaerobic digesters supplemented with carbon cloth had a higher capacity to resist the acidic impacts in mesophilic AD operating at 35°C. The microbial community analysis revealed that *Geobacter* and *Methanosaeta* species were closely attached to the surface of carbon cloth, suggesting that the predominant working mode for the interspecies electron exchange might shift from MIET to DIET (Zhao et al., 2017). Granular activated carbon has been reported to promote the enrichment of microbes utilizing a DIET process, thereby leading to an increase in methane production rate by 77.6% (Lee et al., 2016). Conductive materials were also shown to promote thermophilic AD (~55°C), as evidenced by low volatile fatty acid (VFAs) accumulation, high biomethane production rate, and more robust responses against hydrogen inhibition (Yan et al., 2017). Renewable pyrogenic carbon has shown the capability of directly transferring electrons (Sun et al., 2017), suggesting a cost-effective application of DIET. To illustrate the dynamic advantages of DIET over MIET in AD, simplified models have been proposed to calculate the maximum potential of electric current (Cruz Viggi et al., 2014; Lin et al., 2017; Lin et al., 2018). Cruz Viggi et al. modeled the electron transfer flow in AD of propionate with the addition of magnetite particles (Cruz Viggi et al., 2014). Theoretical calculations revealed that DIET allows electrons to be transferred among syntrophic partners at rates that are substantially higher than those attained via MIET. Similarly, using ethanol as the model substrate, Lin et al. found that graphene-based DIET can sustain a much higher electric current flux, thereby allowing for more efficient electron transfer in a syntrophic mechanism (Lin et al., 2017).

Substrates such as ethanol, glucose, and VFAs have been investigated for establishing DIET with respect to experimental study and model development. The gap in the state of the art is the application of graphene in the promotion of digestion of protein-derived amino acids (such as glycine). This can open up DIET to a range of substrates such as algae, and potentially facilitate the growth of biomethane as a transport fuel. The degradation of glycine in AD is metabolically different from that of substrates that have previously been investigated (such as ethanol and propionate). Glycine is a type of amino acid that widely exists in protein-rich substrates (such as algae). When compared with ethanol/propionate, amino acid presents the amino group ($–NH_2$), which results in a different metabolic pathway in AD. The degradation of glycine requires certain types of amino-acid-degrading bacteria, which can break down amino acid into acetic acid, ammonia, and CO_2. Theoretically this process can lead to the generation of free electrons or hydrogen gas. However, it is unclear if these electrons can be directly used by other microorganisms through DIET. Previous research has demonstrated that various bacteria can degrade ethanol/propionate producing electrons, which can be further consumed by some methanogens. Given that glycine degradation in AD is metabolically different, such a process via DIET necessitates further investigation. Furthermore, the thermodynamic differences of glycine digestion through DIET/MIET remain unclear. The innovation in this article is that it substantially expands the potential range of substrates that could be syntrophically metabolized via DIET and demonstrates for the first time that the AD of amino acids (in this case glycine) could be facilitated by conductive graphene. This can advance the understanding on the theoretical

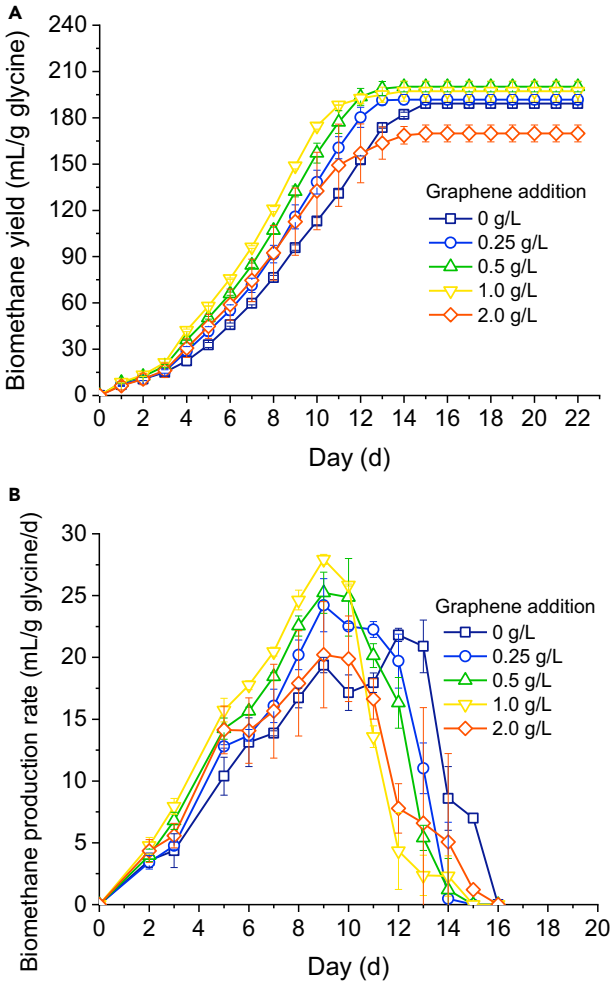


Figure 1. Effects of Graphene Addition on Biomethane Yield and Production Rate from Glycine.
(A) Biomethane yield and (B) biomethane production rate. Data are presented as mean ± standard deviation.

maximum electron transfer via DIET/MIET, and the microbial and functional shift in response to graphene addition in the AD of glycine.

RESULTS AND DISCUSSION

Effects of Graphene Addition on Biomethane Production

Conductive carbonaceous nanomaterials, such as graphene and carbon nanotube, have been assessed to improve the AD of small molecule substrates (such as glucose and ethanol) (Lin et al., 2017; Tian et al., 2017; Li et al., 2015). The metabolic pathways for microbial degradation of carbohydrates and proteins are fundamentally different. Carbohydrates and proteins are the main substrates contributing to biogas production in digestion. Carbohydrates are more favorable as a substrate for microbes than proteins in AD. Protein-derived amino acids may exhibit different metabolic characteristics and digestion performance in the presence of graphene when compared with carbohydrate-derived sugars.

The effects of graphene addition on biomethane yield and production rate of glycine are illustrated in Figures 1A and 1B, respectively. A biomethane yield of 189.3 mL/g was obtained after 16 days of digestion in the absence of graphene. There was a clear trend that illustrated that suitable additions of graphene could result in significant increases in biomethane yields. For example, the addition of 0.5 g/L graphene led to a significant increase ($p < 0.05$) in biomethane yield to 200.1 mL/g. However, further increasing graphene

addition to 2.0 g/L adversely affected the biomethane yield, leading to a decrease to 170.0 mL/g. The higher concentration of graphene led to an inhibition effect on AD, suggesting that cytotoxicity could become a limiting factor when applying graphene nanomaterial in a microbial process. Cytotoxicity induced by several carbon nanomaterials (such as graphene and carbon nanotube) to different microorganisms has been observed in previous studies. For example, Liu et al. investigated the antibacterial effects of graphene-based nanomaterials (including graphene oxide and reduced graphene oxide) on the model bacteria *Escherichia coli* (Liu et al., 2011). The authors proposed a three-step antimicrobial mechanism, which includes initial cell deposition on graphene-based materials, membrane stress caused by direct contact with sharp nanosheets, and the ensuing superoxide anion-independent oxidation (Liu et al., 2011). Pasquini et al. demonstrated that surface functionalization of carbon nanotubes could lead to different antibacterial effects on *Escherichia coli* K12 (Pasquini et al., 2012). The size of nanomaterials is also a key factor that affects the antibacterial effects. Perreault et al. found that graphene-oxide-based surface coatings showed higher antimicrobial activity for smaller sizes (Perreault et al., 2015). It has also been reported that graphene can damage the bacterial cell membrane as a result of direct contact with the very sharp edges of the graphene nanosheets, resulting in an efflux of intracellular components such as RNA (Akhavan and Ghaderi, 2010). The plausible explanation of the antibacterial effect is possibly related to the synergistic impacts of cell membrane perturbation and oxidative stress, but the toxicological mechanisms at the molecular level remain unclear (Qu et al., 2015).

As shown in Figure 1B, the peak biomethane production rate in the absence of graphene was obtained at 12 days with a value of 21.8 mL/g/day. The presence of various graphene concentrations greatly reduced the time for peak production rate from 12 to 9 days. The highest peak biomethane production rate of 27.9 mL/g/day was achieved with the addition of 1.0 g/L graphene, corresponding to an enhancement of 28.0% when compared with the value without graphene addition. These results indicated that the suitable addition of conductive graphene could enable a much quicker digestion process, due to the potential establishment of DIET.

Effects of Graphene Addition on Glycine Conversion in AD

Glycine ($C_2H_5NO_2$), as a typical C_2 amino acid derived from protein-rich substrates (such as microalgae and seaweed), can be used as an electron-donating source for AD. The conversion of glycine in digestion requires the syntrophy of acidogenic bacteria and methanogenic archaea. Table 2 presents the metabolic pathways of glycine conversion and the associated Gibbs free energy changes ($\Delta G_0'$) under standard conditions. For the electron-producing reaction, either MIET or DIET can be employed by diverse acidogenic bacteria. In a similar way, for the electron-consuming reaction, either MIET or DIET can be employed by diverse methanogenic archaea. The connection established between bacteria and archaea contributes to an efficient electron transfer process. DIET can provide additional energy benefits to the syntrophic partners because there is no need to generate metabolites as electron carriers (such as hydrogen), and the subsequent diffusion of electron carrier is unnecessary. From the perspective of thermodynamic change, the $\Delta G_0'$ value of DIET in terms of the electron-donating process is more negative (−60.0 kJ/mol) when compared with that (−33.4 kJ/mol) of MIET, which indicates that the start-up process of glycine degradation via DIET is thermodynamically more favorable and spontaneous.

Graphene addition (1.0 g/L) enhanced glycine conversion during digestion (Figure 2A). As a result, the production of acetate from glycine was concomitantly accelerated (Figure 2B). The acetate concentration gradually increased with the degradation of glycine in digestion, with the peak acetate concentration of 0.89 mg/L observed at 8 days in the presence of 1.0 g/L graphene. In comparison, the peak acetate concentration of 0.93 mg/L was observed at 12 days of digestion in the absence of graphene. The results suggest that graphene was capable of promoting syntrophic reactions between acidogenic bacteria and methanogenic archaea. The enhanced syntrophy led to improved substrate degradation and utilization, namely, glycine degradation and acetate conversion. These results are in agreement with previous work, which demonstrated that the degradation of ethanol in AD was approximately 30% faster upon the addition of graphene (Lin et al., 2017).

Kinetic Analysis

To further evaluate the differences in digestion induced by graphene addition, three types of models were employed to simulate the kinetic patterns of biomethane production (first-order kinetic model,

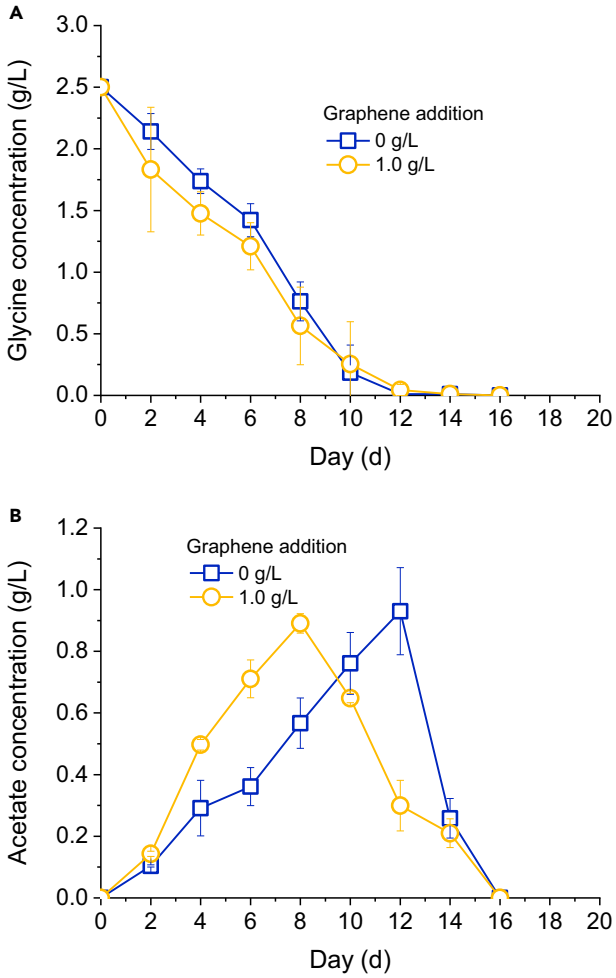


Figure 2. Effects of Graphene Addition on Glycine and Acetate Conversion

(A) Glycine degradation and (B) acetate production and degradation. Data are presented as mean ± standard deviation.

modified Gompertz model, and Cone model, see Table 1). The kinetic parameters, such as P_m, R_m, k, λ, and n were estimated by the studied models (Table 3). According to the results from the first-order kinetic model, there was a significant difference between the measured and predicted biomethane potential ranging from 34.5% to 171.5%, with relatively low correlation coefficients R^2 ranging from 0.9138 to 0.9292. Nonetheless, the first-order kinetic model result suggested that the biomethane production rate constant increased with the addition of graphene from 0 to 1.0 g/L, and then decreased with 2.0 g/L graphene. The highest biomethane production rate constant of 0.0794 (L/d) was observed with the addition of 1.0 g/L graphene.

Comparatively, both the Cone model and the modified Gompertz model exhibited a good fit with the measured data, as evidenced by the high correlation coefficients of R^2 and low RMSE (root-mean-square prediction error) values. For the Cone model, the difference between the measured and predicted biomethane potential ranged from 5.12% to 9.56%. The model predicted that the highest biomethane yield of 207.3 mL/g (5.12% difference from the measured data) was obtained with the addition of 1.0 g/L graphene. Correspondingly, the highest obtained biomethane production rate constant was 0.148 day^{-1} when compared with 0.111 day^{-1} without graphene addition.

In agreement with the results from the Cone model, the modified Gompertz model predicted that the addition of 1.0 g/L graphene produced a biomethane potential of 203.1 mL/g (2.99% difference from the

Model	Equation	Parameters	N
First-order kinetic	$P = P_m(1 - \exp(-kt))$	P_m, k	2
Modified Gompertz	$P = P_m \exp\left\{-\exp\left[\frac{R_m e}{P_m}(\lambda - t) + 1\right]\right\}$	P_m, R_m, λ	3
Cone	$P = \frac{P_m}{1 + (kt)^{-n}}$	P_m, k, n	3

Table 1. Models Used to Describe Biomethane Production from Glycine With/Without Graphene Addition

P_m, maximum biomethane potential (mL/g); k, reaction rate constant (1/d); R_m, peak biomethane production rate (mL/g/day); λ, lag-phase time of biomethane production (d); n, shape factor; N, number of model parameter.

measured data). The peak biomethane production rate was accordingly increased from 20.3 mL/g/day to 26.6 mL/g/day (equivalent to a 31.0% increase). In addition, the Gompertz model gave a lag time of 2.87 days with the addition of 1.0 g/L graphene when compared with 3.88 days in the control condition. Based on the statistical indicators in terms of high correlation coefficient R^2 (0.9895–0.9930) and low RMSE value (5.37–8.31), the modified Gompertz model demonstrated the best fit for the experimental data.

To evaluate the enhancing effects of graphene on AD, the relations of graphene additions (0–1.0 g/L) with different kinetic parameters derived from the modified Gompertz model are presented in Figure 3. A lack of correlation (R^2 = 0.2987) was observed between graphene additions and biomethane yield potentials (Figure 3A). This can be explained by the fact that glycine was completely consumed after AD regardless of graphene addition, resulting in insignificant changes in the overall biomethane yield. Interestingly, apart from the biomethane yield potential, other parameters including the peak biomethane production rate, lag phase time, and peak time exhibited strong positive linear correlations with graphene addition. The best performance was achieved in the presence of 1.0 g/L graphene. Figure 3B shows that the peak biomethane production rate was positively (R^2 = 0.7848) affected by increased graphene addition. Similarly, both lag-phase time (λ) and peak time (T_m) showed a positive linear correlation with graphene addition with R^2 = 0.88337 and 0.96553, respectively (Figures 3C and 3D).

Microbial Taxonomic Patterns in Response to Graphene Addition

In the AD of glycine, bacterial communities are responsible for converting glycine to acetic acid, carbon dioxide, and hydrogen, whereas archaeal communities are responsible for converting acetic acid or carbon dioxide to methane. To better understand the bacterial and archaeal responses to graphene addition, four groups of digestate samples, including the digestate without graphene addition and digestate with 0.25, 0.5, and 1.0 g/L graphene added were analyzed (Figures 4A and 4B).

In the samples without graphene addition, *Levilinea* (18.0%) and *Aminobacterium* (17.6%) were the dominant bacterial genera. It has been reported that *Levilinea* and *Aminobacterium* are capable of fermenting amino acids into VFAs, such as acetate and butyrate, along with the production of hydrogen gas (Yamada et al., 2006; Baena et al., 1998). Taking glycine as an example, the metabolic pathway is described as follows:

$$C_2H_5NO_2 + 2/3H_2O \rightarrow 2/3CH_3COO^- + 2/3H^+ + NH_3 + 2/3CO_2 + 1/3H_2$$

The high abundance of amino-acid-degrading bacteria was ascribed to the adaptation effect of glycine in AD. When compared with the incubation without graphene addition, higher concentrations of graphene gradually decreased the abundance of *Aminobacterium* from 17.6% to 4.9%. However, the presence of 1.0 g/L graphene resulted in significant enrichment of *Sedimentibacter* from 4.7% to 7.8%. Interestingly, *Sedimentibacter*-related species can ferment glycine to acetic acid without production of hydrogen gas (Lechner, 2015), and the metabolic pathway can be described as follows:

$$C_2H_5NO_2 + 2/3H_2O \rightarrow 2/3CH_3COO^- + 4/3H^+ + NH_3 + 2/3CO_2 + 2/3e^-$$

This suggests that the free electrons produced from glycine oxidation have to be consumed by other microorganisms, particularly the methanogens. This further implies the possibility of DIET between fermentative bacteria and methanogenic archaea. *Sedimentibacter* has also been identified in the core

Process	Reaction	$\Delta G_0'$ (kJ/mol)
Electron-producing reaction	1. MIET: $C_2H_5NO_2 + 2/3H_2O \rightarrow 2/3CH_3COO^- + 2/3H^+ + NH_3 + 2/3CO_2 + 1/3H_2$	−33.4
	2. DIET: $C_2H_5NO_2 + 2/3H_2O \rightarrow 2/3CH_3COO^- + 4/3H^+ + NH_3 + 2/3CO_2 + 2/3e^-$	−60.0
Electron-consuming reaction	3. MIET: $1/3H_2 + 1/12CO_2 \rightarrow 1/12CH_4 + 1/6H_2O$	−10.9
	4. DIET: $2/3H^+ + 2/3e^- + 1/12CO_2 \rightarrow 1/12CH_4 + 1/6H_2O$	15.7
Acetate-consuming reaction	$2/3CH_3COO^- + 2/3H^+ \rightarrow 2/3CH_4 + 2/3CO_2$	−23.9
Overall	$C_2H_5NO_2 + 1/2H_2O \rightarrow 3/4CH_4 + NH_3 + 5/4CO_2$	−68.2

Table 2. Reactions and Changes in Gibbs Free Energy Values for Glycine Conversion to Methane with Different Pathways

MIET, mediated interspecies electron transfer; DIET, direct interspecies electron transfer. Values are calculated at different temperatures under standard conditions (1 M concentration of all solutes, 25°C, 1 atm, and neutral pH). Negative value indicates that the reaction is thermodynamically favorable and proceeds spontaneously.

community for microbial fuel cell systems fed with swine manure, due to their exoelectrogenic role with high power generation capability (Vilajeliu-Pons et al., 2016).

The structure of the archaeal community in response to graphene addition is shown in Figure 4B. When graphene is absent, the genera of *Methanobacterium* and *Methanosaeta* are dominant in the archaeal community, accounting for 61.7% and 31.2%, respectively. Most species of *Methanobacterium* are recognized as hydrogen-consuming methanogens, converting carbon dioxide and hydrogen into methane. However, a previous study revealed that specific species of *Methanobacterium* can directly receive electrons for electro-methanogenesis, in which *Methanobacterium palustre* accounted for 86.7% of the total cells (Cheng et al., 2009). This finding suggests that methanogens can directly accept electrons, and builds further support for interspecies electron transfer. *Methanosaeta* are mainly acetate-consuming methanogens, which cleave acetic acid into methane and carbon dioxide. When increasing the graphene addition to 1.0 g/L in the digestion, the abundance of *Methanosaeta* decreased to 16.8%, compared with 31.2% without graphene addition. In contrast, the abundance of *Methanosarcina* gradually increased from 6.5% (without graphene addition) to 11.3% (1.0 g/L graphene addition). *Methanosarcina* are known as the most metabolically diverse methanogens. Recent studies have demonstrated that some species (such as *Methanosarcina barkeri*) are capable of directly receiving electrons from electroactive bacteria (such as *Geobacter*) for CO_2 reduction (Rotaru et al., 2014a). The increase in abundance of *Methanosarcina* after graphene addition suggests their likely participation in the DIET process ($2/3H^+ + 2/3e^- + 1/12CO_2 \rightarrow 1/12CH_4 + 1/6H_2O$). In the present study, the enrichment of archaea *Methanosarcina* and *Methanobacterium* in response to graphene addition proposes a possibility that they may play an important role in conducting DIET.

Potential Microbial Network for Glycine Degradation in AD

AD is known to require multiple groups of microorganisms working together to convert organic substrates to methane. The complete degradation of glycine involves the cooperation of acidogenic bacteria and methanogenic archaea. Acidogenic bacteria are responsible for converting glycine to acetic acid and producing electrons (or hydrogen), whereas methanogenic archaea are capable of converting acetic acid, carbon dioxide, and electrons to methane through three major pathways, acetoclastic methanogenesis, hydrogenotrophic methanogenesis, and DIET methanogenesis.

Based on the differences in microbial community structure (Figure 4) and the metabolic functions of the bacterial genera present, a potential microbial network of the major bacteria and archaea involved in the AD of glycine is illustrated in Figure 5. In the AD of glycine in the absence of graphene, glycine is first degraded by acidogenic bacteria, which may include *Levilinea* (18.0%) and *Aminobacterium* (17.6%), as shown in Figure 5A. Glycine acidification may then lead to the production of intermediate products such as acetic acid and hydrogen (or protons and electrons). The further production of methane will then

Model	Parameter	Graphene Addition (g/L)				
		0	0.25	0.5	1.0	2.0
First-order	$P_{measured}$ (mL/g)	189.3	191.8	200.1	197.2	169.9
	P_m (mL/g)	513.9	332.6	303.7	265.3	256.0
	Difference (%)	171.5	73.4	51.8	34.5	50.7
	k (1/d)	0.0249	0.0482	0.0613	0.0794	0.0616
	Adjusted R^2	0.9260	0.9138	0.9188	0.9185	0.9292
	RMSE (mL/g)	20.5	22.5	22.4	21.8	17.5
Cone	$P_{measured}$ (mL/g)	189.3	191.8	200.1	197.2	169.9
	P_m (mL/g)	207.4	204.1	212.6	207.3	181.3
	Difference (%)	9.56	6.41	6.25	5.12	6.71
	k (1/d)	0.111	0.126	0.134	0.148	0.135
	n	3.44	3.69	3.49	3.47	3.25
	Adjusted R^2	0.9879	0.9866	0.9870	0.9875	0.9907
	RMSE (mL/g)	8.28	8.87	8.96	8.52	6.35
Modified Gompertz	$P_{measured}$ (mL/g)	189.3	191.8	200.1	197.2	169.9
	P_m (mL/g)	201.4	200.2	207.9	203.1	176.2
	Difference (%)	6.39	4.38	3.90	2.99	3.71
	R_m (mL/g/day)	20.3	23.8	25.1	26.6	20.4
	λ (d)	3.88	3.62	3.19	2.87	2.95
	Adjusted R^2	0.9895	0.9882	0.989	0.990	0.9930
	RMSE (mL/g)	7.71	8.31	8.10	7.52	5.37

Table 3. Estimated Parameters from the First-Order Kinetic, Modified Gompertz, and Cone Models Simulating Biomethane Production from Glycine
P_m, maximum biomethane potential (mL/g); k, reaction rate constant (1/d); R_m, peak biomethane production rate (mL/g/day); λ, lag-phase time of biomethane production (d); n, shape factor; N, number of model parameter; RMSE, root-mean-square prediction error.

primarily depend on the acetoclastic and hydrogenotrophic pathways for methanogenesis, with acetic acid being utilized by *Methanosaeta* (31.2%) to produce methane and carbon dioxide. Carbon dioxide may then be reduced to methane by *Methanobacterium* (61.7%) and *Methanosarcina* (6.6%) through the hydrogenotrophic pathway.

The presence of conductive graphene in the digestion process appears to markedly change the syntrophic interactions between the acidogenic bacteria and methanogenic archaea (Figure 5B). *Levilinea* (17.8%) remained as the dominant acidogenic bacteria, whereas *Sedimentibacter* (7.8%) was enriched and is likely to have played an important role in degrading glycine. As previously mentioned, *Sedimentibacter* are capable of converting glycine to acetic acid and free electrons. Archaea *Methanobacterium* (61.7%) and *Methanosarcina* (11.3%) are capable of utilizing free electrons for carbon dioxide reduction. Therefore, the enrichment of these microorganisms in methanogenesis proposes a possibility that they may play an important role in conducting DIET.

Comparison of Maximum Electron Transfer for MIET and Graphene-Based DIET

Microbial electron transfer between electron-producing acidogens and electron-consuming methanogens in AD might proceed via either DIET or MIET (with hydrogen as an electron carrier). To compare the electron transfer efficiencies of DIET and MIET, previous models have been proposed based on the Nernst equation and Fick's diffusion law (Cruz Viggi et al., 2014; Lin et al., 2017; Lin et al., 2018).

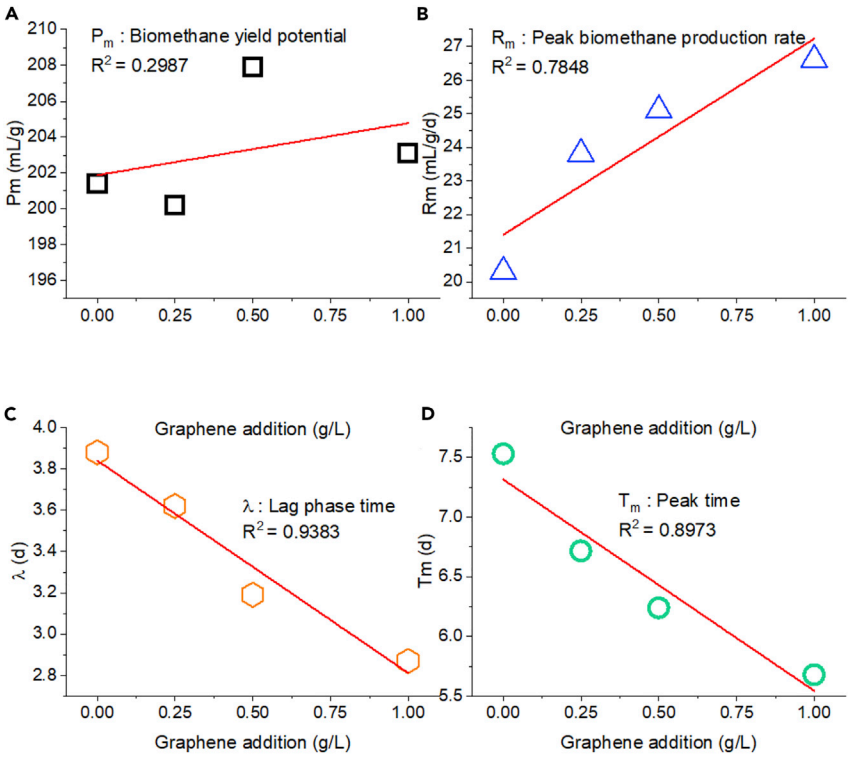


Figure 3. Correlations of Graphene Addition with Different Kinetic Parameters in Anaerobic Digestion

(A) Biomethane yield potential (P_m), (B) peak biomethane production rate (R_m), (C) lag phase time (λ), and (D) peak time (defined as $T_m = P_m/R_m/e + \lambda$).

Using ethanol as the substrate in AD, Lin et al. found that graphene-based DIET can sustain a much higher electric current flux than hydrogen transfer, thereby allowing for more efficient electron transfer via the syntrophic mechanism (Lin et al., 2017). Substrates such as ethanol, glucose, and VFAs have been investigated for establishing DIET in AD. The present study increased the range of substrates known to be syntrophically metabolized via DIET and demonstrated for the first time that the AD of amino acid (glycine) could be facilitated by conductive graphene. The degradation of glycine in AD was metabolically different than those of the previous substrates investigated, such as ethanol and propionate. Therefore, to further reveal the difference of maximum electron transfer achieved by DIET and MIET, the simplified calculations were proposed based on the Nernst equation and Fick's diffusion law.

The maximum electron transfer for MIET in AD of glycine was calculated based on Fick's diffusion law (see Figure S2, Supplemental Information). The maximum driving force for hydrogen diffusion depends on the highest hydrogen concentration generated by acidogenic bacteria and the lowest hydrogen concentration reached by methanogenic archaea. The highest hydrogen concentration was calculated in terms of the electron-donating reaction (Table 2, $C_2H_5NO_2 + 2/3H_2O \rightarrow 2/3CH_3COO^- + 2/3H^+ + NH_3 + 2/3CO_2 + 1/3H_2$, corresponding to $\Delta G' = 0$), and the lowest hydrogen concentration was calculated in terms of the electron-consuming reaction (Table 2, $1/3H_2 + 1/12CO_2 \rightarrow 1/12CH_4 + 1/6H_2O$, corresponding to $\Delta G' = 0$). To estimate the maximum hydrogen flux in DIET, the concentrations of reactants and products were set identical to those in MIET (see Figure S1, Supplemental Information). Assuming that the electrons are released from glycine degradation through the electron-donating reaction (Table 2, $C_2H_5NO_2 + 2/3H_2O \rightarrow 2/3CH_3COO^- + 4/3H^+ + NH_3 + 2/3CO_2 + 2/3e^-$, $\Delta G^{0\prime} = -60.0$ kJ/mol), the electrons are directly transferred to methanogens via graphene. Methanogens reduce CO_2 to CH_4 through the electron-consuming reaction (Table 2, $2/3H^+ + 2/3e^- + 1/12CO_2 \rightarrow 1/12CH_4 + 1/6H_2O$, $\Delta G^{0\prime} = 15.7$ kJ/mol). The maximum driving force for electron transfer is given by the redox potential (ΔE) of the overall reaction ($C_2H_5NO_2 + 1/2H_2O \rightarrow 1/12CH_4 + 2/3CH_3COO^- + 2/3H^+ + NH_3 + 7/12CO_2$, $\Delta G^{0\prime} = -44.3$ kJ/mol).

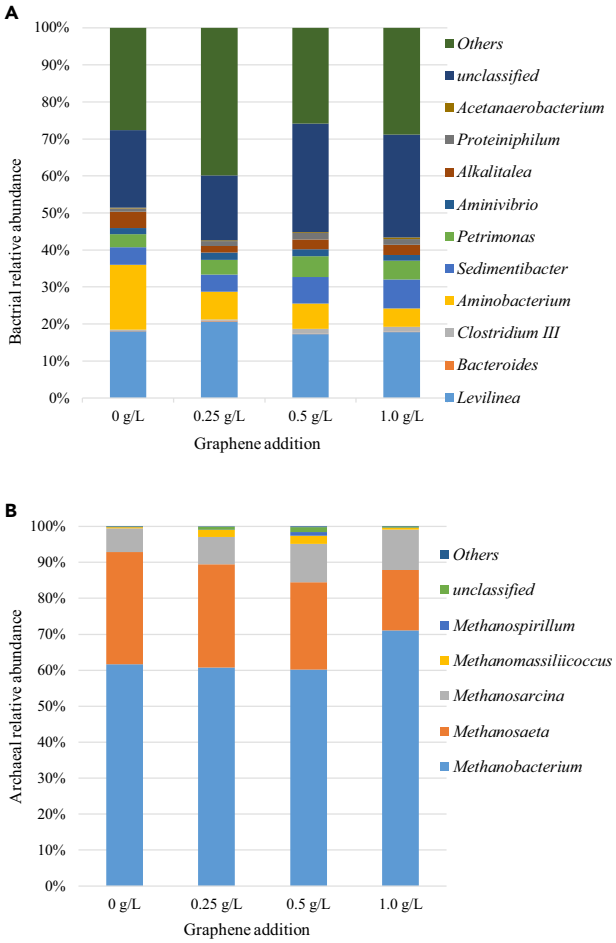


Figure 4. Microbial Community Structures at Genus Level with/without Graphene Addition after Anaerobic Digestion of Glycine

(A) Bacterial and (B) archaeal communities. Genera with less than 1% abundances are classified as "others."

The resulting maximum electron flux via MIET and graphene-based DIET was calculated as 9.8 nA and 4.1 mA, respectively. The result demonstrated that the two electron transfer mechanisms could lead to a huge difference in maximum electron transfer flux. This is in accordance with previous studies (Cruz Viggi et al., 2014; Lin et al., 2017), in which DIET showed a clear advantage over MIET in maximum electron transfer when converting propionate and ethanol in AD.

Conclusions

This study demonstrated that graphene nanomaterial can promote AD of protein-derived glycine. The addition of 1.0 g/L graphene led to the highest peak biomethane production rate of 27.9 mL/g/day, which was 28.0% higher than that without graphene addition. It was observed that the consumption of glycine was enhanced simultaneously. Compared with the first-order kinetic model and the Cone model, the modified Gompertz model exhibited the best fit with measured data, and indeed a higher graphene addition (2.0 g/L) had a toxic effect on digestion. The analysis of kinetic parameters revealed that the peak biomethane production rate, lag-phase time, and peak time showed strong linear correlations with graphene additions from 0.25 to 1.0 g/L. The improved performance may be attributed to the potential establishment of DIET between *Sedimentibacter* (7.8% in abundance) and *Methanosarcina* (11.3%).

EU policies require a significant rise in advanced biofuels (such as biomethane) in the share of renewable energy consumption. The deployment of the proposed AD systems can help to meet this target. Although

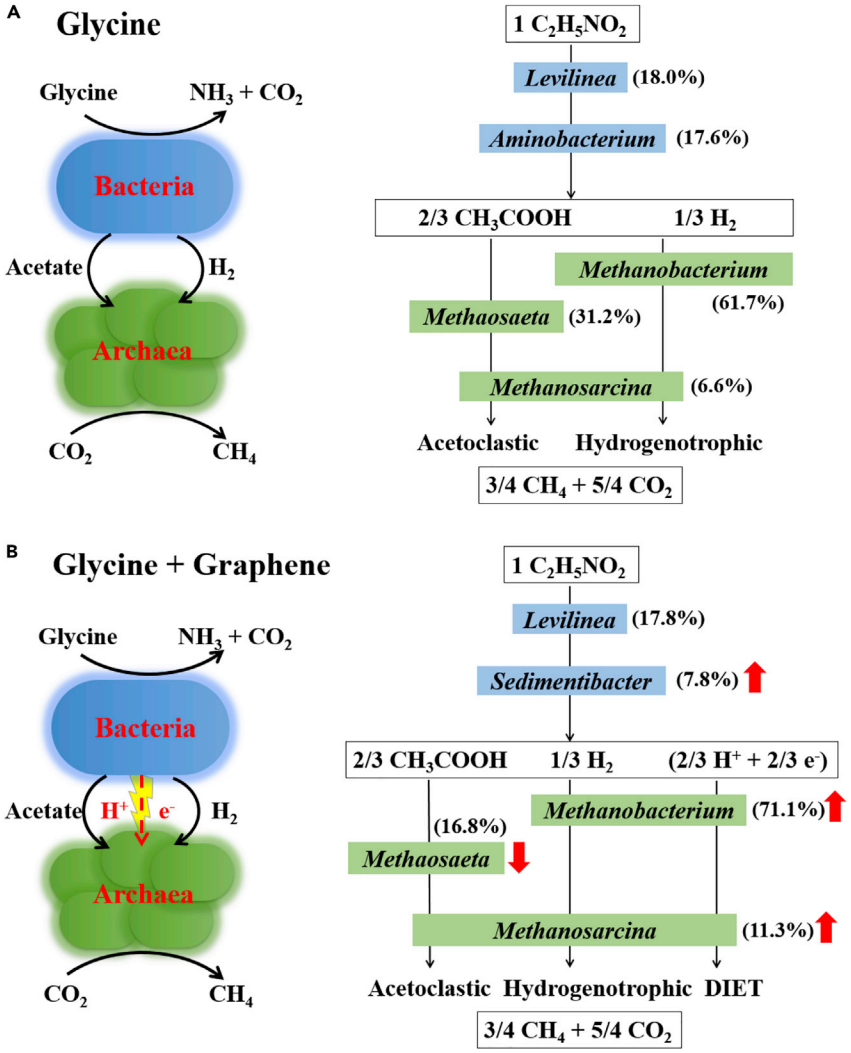


Figure 5. Microbial Community Structures at Genus Level with/without Graphene Addition after Anaerobic Digestion of Glycine

(A) Without graphene addition and (B) with 1.0 g/L graphene addition. The numbers in brackets indicate the abundance of microorganisms.

the direct use of high-cost nanomaterials in AD is unlikely to be economically feasible, the proof of concept benefits the application of DIET to promoting biomethane production from a variety of feedstock. Biochar derived from thermochemical processing of biomass may be a cost-effective alternative to graphene. Biochar produced under certain conditions can exhibit outstanding electron transfer capability. In a similar manner to graphene, high-quality biochar may enable the establishment of DIET-based AD. Biochar can act as a bridge linking biological AD and thermochemical pyrolysis. The enhanced AD system through addition of inexpensive materials can improve biogas production efficiency, thereby potentially reducing the cost of systems deployment.

Limitations of Study

One limitation of the bioenergy system using nanomaterials apparently is the high cost. Future work is required to propose an economically viable bioenergy system incorporating recyclable conductive materials (such as high-quality biochar). Effective bioreactor design improving biomethane production efficiency is also necessary to facilitate the deployment of the integrated AD system. Deep microbial analysis should be performed to further reveal the specific microorganisms involved in the DIET process.

METHODS

All methods can be found in the accompanying Transparent Methods supplemental file.

SUPPLEMENTAL INFORMATION

Supplemental Information includes Transparent Methods and two figures and can be found with this article online at https://doi.org/10.1016/j.isci.2018.11.030.

ACKNOWLEDGMENTS

R.L. gratefully acknowledges the support from the European Union's Horizon 2020 research and innovation program under the Marie Skłodowska-Curie grant (No. 797259). This collaborative Irish Chinese study was co-funded by Science Foundation Ireland (SFI) through the Centre for Marine and Renewable Energy (MaREI) under Grant No. 12/RC/2302 and 16/SP/3829 and by the National Key Research and Development Program-China (2016YFE0117900). This work was also funded by Zhejiang Provincial Key Research and Development Program-China (2017C04001). Industrial co-funding from ERVIA and Gas Networks Ireland (GNI) through the Gas Innovation Group is gratefully acknowledged. A.X. is funded by the National Science Foundation for Young Scientists of China (No. 51606021).

AUTHOR CONTRIBUTIONS

R.L. designed the anaerobic digestion experiments. C.D. and J.C. helped analyze the results on bio-methane production. S.A.J. checked the microbial section and uploaded the sequence data. R.L. was the first author providing the first version of the manuscript. A.X., P.N.L.L., A.D.W.D., and J.D.M. reviewed, edited and polished the manuscript.

DECLARATION OF INTERESTS

The authors declare no competing interests.

Received: August 30, 2018
Revised: November 6, 2018
Accepted: November 16, 2018
Published: December 21, 2018

REFERENCES

Akhavan, O., and Ghaderi, E. (2010). Toxicity of graphene and graphene oxide nanowalls against bacteria. ACS Nano *4*, 5731–5736.

Ariunbaatar, J., Panico, A., Esposito, G., Pirozzi, F., and Lens, P.N.L. (2014). Pretreatment methods to enhance anaerobic digestion of organic solid waste. Appl. Energy *123*, 143–156.

Baena, S., Fardeau, M.L., Labat, M., Ollivier, B., Thomas, P., Garcia, J.L., and Patel, B.K.C. (1998). *Aminobacterium colombiensegen.* nov. sp. nov., an amino acid-degrading anaerobe isolated from anaerobic sludge. Anaerobe *4*, 241–250.

Batstone, D.J., and Virdis, B. (2014). The role of anaerobic digestion in the emerging energy economy. Curr. Opin. Biotechnol. *27*, 142–149.

Cheng, S., Xing, D., Call, D.F., and Logan, B.E. (2009). Direct biological conversion of electrical current into methane by electromethanogenesis. Environ. Sci. Technol. *43*, 3953–3958.

Cruz Viggi, C., Rossetti, S., Fazi, S., Paiano, P., Majone, M., and Aulenta, F. (2014). Magnetite particles triggering a faster and more robust syntrophic pathway of methanogenic propionate degradation. Environ. Sci. Technol. *48*, 7536–7543.

European Biogas Association. 2016. 6th Edition of the Statistical Report on European Anaerobic Digestion Industry and Markets. Available at: http://european-biogas.eu/2016/12/21/eba-launches-6th-edition-of-the-statistical-report-of-the-european-biogas-association/.

European Commission. Proposal for a Directive of the European Parliament and of the Council on the Promotion of the Use of Energy from Renewable Sources (Recast) 2016; 382. Available at: https://eur-lex.europa.eu/legal-content/EN/ALL/?uri=COM%3A2016%3A767%3AFIN.

FitzGerald, J.A., Allen, E., Wall, D.M., Jackson, S.A., Murphy, J.D., and Dobson, A.D. (2015). *Methanosarcina* play an important role in anaerobic co-digestion of the seaweed *Ulva lactuca*: taxonomy and predicted metabolism of functional microbial communities. PLoS One *10*, e0142603.

International Energy Agency (IEA). Energy Technology Perspectives 2017. Available in: http://www.iea.org/etp2017/summary/.

Lechner, U. (2015). Sedimentibacter. Bergey's Manual of Systematics of Archaea and Bacteria (John Wiley & Sons, Ltd).

Lee, J.-Y., Lee, S.-H., and Park, H.-D. (2016). Enrichment of specific electro-active microorganisms and enhancement of methane production by adding granular activated carbon in anaerobic reactors. Bioresourc. Technol. *205*, 205–212.

Li, L.-L., Tong, Z.-H., Fang, C.-Y., Chu, J., and Yu, H.-Q. (2015). Response of anaerobic granular sludge to single-wall carbon nanotube exposure. Water Res. *70*, 1–8.

Lin, R., Cheng, J., Zhang, J., Zhou, J., Cen, K., and Murphy, J.D. (2017). Boosting biomethane yield and production rate with graphene: the potential of direct interspecies electron transfer in anaerobic digestion. Bioresourc. Technol. *239*, 345–352.

Lin, R., Cheng, J., Ding, L., and Murphy, J.D. (2018). Improved efficiency of anaerobic digestion through direct interspecies electron transfer at mesophilic and thermophilic temperature ranges. Chem. Eng. J. *350*, 681–691.

Liu, S., Zeng, T.H., Hofmann, M., Burcombe, E., Wei, J., Jiang, R., Kong, J., and Chen, Y. (2011). Antibacterial activity of graphite, graphite oxide, graphene oxide, and reduced graphene oxide: membrane and oxidative stress. ACS Nano *5*, 6971–6980.

Mei, R., Narihiro, T., Nobu, M.K., Kuroda, K., and Liu, W.-T. (2016). Evaluating digestion efficiency in full-scale anaerobic digesters by identifying active microbial populations through the lens of microbial activity. Sci. Rep. *6*, 34090.

Pasquini, L.M., Hashmi, S.M., Sommer, T.J., Elimelech, M., and Zimmerman, J.B. (2012). Impact of surface functionalization on bacterial cytotoxicity of single-walled carbon nanotubes. Environ. Sci. Technol. *46*, 6297–6305.

Perreault, F., de Faria, A.F., Nejati, S., and Elimelech, M. (2015). Antimicrobial properties of graphene oxide nanosheets: why size matters. ACS Nano *9*, 7226–7236.

Qu, Y., Ma, Q., Deng, J., Shen, W., Zhang, X., He, Z., van Nostrand, J.D., Zhou, J., and Zhou, J. (2015). Responses of microbial communities to single-walled carbon nanotubes in phenol wastewater treatment systems. Environ. Sci. Technol. *49*, 4627–4635.

Rotaru, A.-E., Shrestha, P.M., Liu, F., Markovaite, B., Chen, S., Nevin, K., and Lovley, D. (2014a). Direct interspecies electron transfer between *Geobacter metallireducens* and *Methanosarcina barkeri*. Appl. Environ. Microbiol. *80*, 4599–4605.

Rotaru, A.-E., Shrestha, P.M., Liu, F., Shrestha, M., Shrestha, D., Embree, M., Zengler, K., Wardman, C., Nevin, K.P., and Lovley, D.R. (2014b). A new model for electron flow during anaerobic digestion: direct interspecies electron transfer to *Methanosaeta* for the reduction of carbon dioxide to methane. Energy Environ. Sci. *7*, 408–415.

Sun, T., Levin, B.D., Guzman, J.J., Enders, A., Muller, D.A., Angenent, L.T., and Lehmann, J. (2017). Rapid electron transfer by the carbon matrix in natural pyrogenic carbon. Nat. Commun. *8*, 14873.

Tian, T., Qiao, S., Li, X., Zhang, M., and Zhou, J. (2017). Nano-graphene induced positive effects on methanogenesis in anaerobic digestion. Bioresourc. Technol. *224*, 41–47.

Vilajeliu-Pons, A., Bañeras, L., Puig, S., Molognoni, D., Vilà-Rovira, A., Hernández-del Amo, E., Balaguer, M.D., and Colprim, J. (2016). External resistances applied to MFC affect core microbiome and swine manure treatment efficiencies. PLoS One *11*, e0164044.

Xia, A., Cheng, J., and Murphy, J.D. (2016). Innovation in biological production and upgrading of methane and hydrogen for use as gaseous transport biofuel. Biotechnol. Adv. *34*, 451–472.

Xu, J., Hao, J., Guzman, J.J., Spirito, C.M., Harroff, L.A., and Angenent, L.T. (2018). Temperature-phased conversion of acid whey waste into medium-chain carboxylic acids via lactic acid: no external e-donor. Joule *2*, 280–295.

Yamada, T., Sekiguchi, Y., Hanada, S., Imachi, H., Ohashi, A., Harada, H., and Kamagata, Y. (2006). *Anaerolinea thermolimosa* sp. nov., *Levilinea saccharolytica* gen. nov., sp. nov. and *Leptolinea tardivitalis* gen. nov., sp. nov., novel filamentous anaerobes, and description of the new classes Anaerolineae classis nov. and Caldilineae classis nov. in the bacterial phylum Chloroflexi. Int. J. Syst. Evol. Microbiol. *56* (Pt 6), 1331–1340.

Yan, W., Shen, N., Xiao, Y., Chen, Y., Sun, F., Kumar Tyagi, V., and Zhou, Y. (2017). The role of conductive materials in the start-up period of thermophilic anaerobic system. Bioresourc. Technol. *239*, 336–344.

Yin, Q., Yang, S., Wang, Z., Xing, L., and Wu, G. (2018). Clarifying electron transfer and metagenomic analysis of microbial community in the methane production process with the addition of ferroferric oxide. Chem. Eng. J. *333*, 216–225.

Zhao, Z., Zhang, Y., Li, Y., Dang, Y., Zhu, T., and Quan, X. (2017). Potentially shifting from interspecies hydrogen transfer to direct interspecies electron transfer for syntrophic metabolism to resist acidic impact with conductive carbon cloth. Chem. Eng. J. *313*, 10–18.

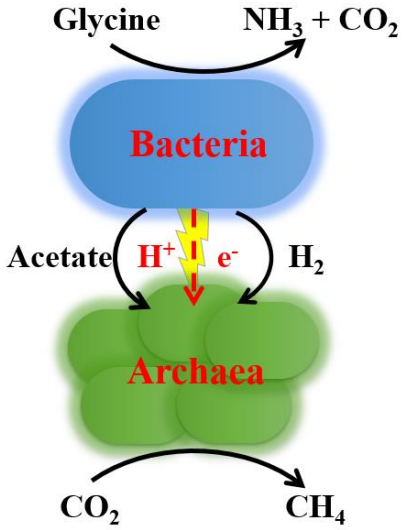
ISCI, Volume *10*

Supplemental Information

Graphene Facilitates Biomethane Production from Protein-Derived Glycine in Anaerobic Digestion

Richen Lin, Chen Deng, Jun Cheng, Ao Xia, Piet N.L. Lens, Stephen A. Jackson, Alan D.W. Dobson, and Jerry D. Murphy

Supporting Information



$$i = \sigma \bullet \frac{S_{conduit}}{d} \bullet (E_{met} - E_{ace})$$

i=Electric current associate with electron carrier flux

σ=Electrical conductivity of graphene

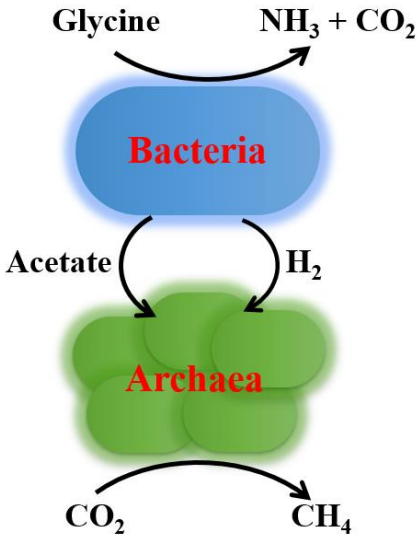
$S_{conduit}$=Cross-sectional area of the electron conduit

d=Distance between cells

E_{met}=Redox potential of ethanol oxidation reaction

E_{ace}=Redox potential of CO_2 reduction reaction

Figure S1. Calculation of maximum electron flux for graphene-based direct interspecies electron transfer (DIET) between acidogenic bacteria and methanogenic archaea, related to Table 2



$$i = D_f \bullet \frac{S_{cell}}{d} \bullet ([H_2]_{highest} - [H_2]_{lowest}) \bullet n \bullet F$$

i=Electric current associate with electron carrier flux

D_f=Diffusion coefficient of H_2 in water

S_{cell}=Surface area of the cells

d=Distance between cells

$[H_2]_{highest}$=Highest H_2 concentration produced by acetogen

$[H_2]_{lowest}$=Lowest H_2 concentration reached by methanogen

n=mol of electrons per mol of H_2

F=Faraday's constant

Figure. S2 Calculation of maximum electron flux for interspecies hydrogen transfer (MIET) between acidogenic bacteria and methanogenic archaea, related to Table 2

Transparent Methods

Inoculum

The inoculum for biomethane potential (BMP) assays was sourced from lab-scale continuous stirred-tank reactors, which are operated at 35 °C. The lab reactors were fed with various feedstocks such as seaweed, grass and animal slurry. The inoculum was kept at 35 °C in a water bath, while being fed once a week with cellulose as a carbon source (organic loading rate of 1.0 g/L/d). Prior to the BMP experiments, the inoculum was degassed for two weeks. The total solid (TS) content of the inoculum was 2.38 wwt%, and the volatile solid (VS) content was 1.34 wwt%.

Biomethane potential assays

Batch experiments of AD were carried out in triplicate in the AMPTS II system (Bioprocess Control, Sweden). The BMP system has the capacity to accommodate 15 glass fermenters (each has a total volume of 650 mL with a working volume of 400 mL). Five experimental groups were designed based on the additions of graphene (0, 0.25, 0.5, 1.0 and 2.0 g/L) in anaerobic digestion. In BMP assays, 150 mL of inoculum (containing 2.0 g VS) were added to each bottle. Subsequently, 1.0 g of amino acid glycine as the substrate were added to each glass fermenter to effect an inoculum to substrate ratio of 2:1. The final liquid volume in each bottle was adjusted to 400 mL with distilled water. Afterwards, all fermenter were sealed, purged with nitrogen gas for 5 min, and maintained at 35 °C in water bath. The biomethane volume was automatically recorded by the AMPST II system (Lin et al., 2018).

Analytic methods

The VS and TS content of the anaerobic inoculum was analyzed by drying of the sample for 24 h

at 105 °C. The ash content was calculated based on the method of subsequent heating for 2 h at 550 °C (Lin et al., 2018). The soluble metabolic products (mainly acetic acid) was characterized through a gas chromatography system (GC; Agilent 7890A, USA) equipped with a flame ionization detector and a DB-FFAP column (Lin et al., 2018). Before injecting to the GC, the liquid samples were first centrifuged at 5000 rpm for 5 min and then adjusted with orthophosphoric acid to a pH value of 2.0. All of the trials and measurements were conducted in triplicate.

To identify the microbial communities in response to different addition levels of graphene, the digestate samples were taken at the end of the digestion period and further analysed. The samples of digestates were rinsed with phosphate-buffered saline, centrifuged for 10 min at 4 °C, and then stored at −20 °C until further processing. The procedures of identifying the bacterial and archaeal communities were as follows. DNA was extracted following the manufacturer's protocol (Omega Bio-Tec, China). PCR amplicon libraries were generated using primers spanning the V3-V4 hypervariable region of the 16S rRNA gene. All PCR reactions from each sample were performed in duplicate in order to minimize bias. The products were checked on 2% agarose gels to determine the success of amplification. Duplicate amplicon samples were pooled together in equal proportions based on their molecular weight and DNA concentrations, purified using calibrated Ampure XP beads and sequenced using the Illumina Miseq platform (Illumina, USA) (Sangon Biotech Shanghai, China). Final operational taxonomic units (OTUs) were taxonomically classified using BLASTN against a curated database derived from RDP. The raw metagenomics datasets have been deposited into the NCBIs sequence Read Archive with the access number SRP158026.

Calculations

Understanding the kinetics of biomethane production is important when evaluating the digestion performance and designing the digester. Three types of models including first-order kinetic model, modified Gompertz model, and Cone model were employed to simulate and compare the kinetic patterns of the biomethane yield from digestion of glycine (Table 1). The kinetic parameters (such as P_m, R_m, k, and λ) were estimated by fitting the BMP data into the models via Origin 8.5 software. The Root Mean Square Prediction Error (RMSE) was calculated to evaluate the accuracy of each model. Statistical analysis of variance (one-way ANOVA) was carried out using Origin 8.5 software to test the impact of graphene addition on the biomethane production. The value of $p < 0.05$ was considered to be statistically significant.

The calculations of theoretical interspecies electron transfer via MIET and DIET are based on the models proposed in a previous study (Lin et al., 2017). The maximum electron transfer flux for graphene-based DIET was calculated using the Ohm's law and Nernst equation as described in Eq. 1:

$$i = \sigma \cdot \frac{S_{conduit}}{d} \cdot (E_{Met} - E_{Ace}) \quad (1)$$

where i is the electron transfer flux, σ is the electrical conductivity of graphene, $S_{conduit}$ is the cross sectional area of the electron conduit, d is the distance between cells, E_{Met} is the redox potential of the glycine oxidation reaction, and E_{Ace} is the redox potential of the carbon dioxide reduction reaction. $\Delta E = E_{Met} - E_{Ace}$ can be determined using the following Eq. 2:

$$\Delta E = E_{Met} - E_{Ace} = \frac{\Delta G'}{nF} \quad (2)$$

where ΔE (V) is the maximum redox potential of the overall reaction for glycine oxidation and carbon dioxide reduction, n is mole electron per reaction, and F is the Faraday's constant. $\Delta G'$ can be calculated according to Eq. 3:

$$\Delta G' = \Delta G^{0'} + RTln\frac{[Acetate]^{2/3} \cdot pCH_4^{1/12} \cdot pNH_3 \cdot pCO_2^{7/12}}{[Gly]} \quad (3)$$

where $\Delta G^{0'}$ (kJ/mol) is the standard Gibbs free energy change per reaction, R = 8.315 J/(mol·K), [Acetate] and [Gly] are the concentrations of acetic acid and glycine in the reaction, pCH_4, pNH_3 and pCO_2 are the concentrations of methane, ammonia and carbon dioxide in the reaction, and T is the reaction temperature.

To determine the maximum electron transfer flux via MIET, the Fick's diffusion law was used to calculate the rate of hydrogen diffusion from bacteria to methanogens (Eq. 4):

$$i = D_f \cdot \frac{S_{cell}}{d} \cdot ([H_2]_{highest} - [H_2]_{lowest}) \cdot n \cdot F \quad (4)$$

where i is the electron transfer flux, D_f is the diffusion constant of hydrogen in water, S_{cell} is the surface area of the cells, d is the distance of between cells, n is mole electron per reaction, F is Faraday's constant, $[H_2]_{highest}$ is the highest hydrogen concentration produced by acetogens, and $[H_2]_{lowest}$ is the lowest hydrogen concentration reached by methanogens. The highest and lowest hydrogen concentration was calculated in terms of the electron-donating reaction and electron-consuming reaction, respectively.

The following parameters were used to determine the thermodynamic values: Glycine concentration ([Gly]) of 7.52 mM, acetate concentration ([Acetate]) of 14.85 mM, CH_4 partial pressure (pCH_4) of 0.6 atm, CO_2 partial pressure (pCO_2) of 0.35 atm, and NH_3 partial pressure (pNH_3) of 0.04 atm. An interbacterial distance (d) of 0.5 μm was assumed with cells (both bacteria and archaea) having a cylindrical shape (assuming diameter = 0.5 μm, length = 2.5 μm). The electrical conductivity of graphene (σ) was determined typically as 850 S/cm. Graphene conduit is assumed as a cuboid shape with a thickness of 16 nm and a length of 2 μm.

The maximum driving force for direct electron transfer is given by the redox potential (ΔE =

$\Delta E_{met} - \Delta E_{ace}$) of the overall reaction ($C_2H_5NO_2 + 1/2H_2O \rightarrow 1/12CH_4 + 2/3CH_3COO^- + 2/3H^+ + NH_3 + 7/12CO_2$, $\Delta G^{0\prime} = -44.3$ kJ/mol). ΔE is determined by Nernst equation $\Delta E = -\Delta G'/nF$ (n = mole electron per reaction, F is Faraday's constant), where $\Delta G'$ can be calculated according to Eq. S1:

$$\Delta G' = \Delta G^{0\prime} + RTln\frac{[Acetate]^{2/3} \cdot pCH_4^{1/12} \cdot pNH_3 \cdot pCO_2^{7/12}}{[Gly]} \quad \text{(Eq. S1)}$$

In which $R = 0.00831451$ kJ/mol/K, and $T = 308.15$ K. The calculated $\Delta G' = -48.92$ kJ/mol. By using Nernst equation, ΔE can be calculated as 0.761 V. By further using equation in Fig. S1, the maximum electron transfer flux of DIET can be obtained as 4.1×10^{-3} A.

To estimate the maximum electron transfer flux in MIET, the concentrations of reactants and products and boundary conditions were set identical to those in DIET. The diffusion constant of H_2 in water at 35 °C was determined as 5.9×10^{-5} cm^2/ s. Fick's diffusion law is used to compute the rate of H_2 diffusion from bacteria to archaea. The highest H_2 concentration was calculated in terms of the electron-donating reaction ($C_2H_5NO_2 + 2/3H_2O \rightarrow 2/3CH_3COO^- + 2/3H^+ + NH_3 + 2/3CO_2 + 1/3H_2$, corresponding to $\Delta G' = 0$). The highest hydrogen partial pressure in practice can be achieved as 1 mM (Stams et al., 2006).

In a similar way, the lowest H_2 concentration was calculated in terms of the electron-consuming reaction ($1/3H_2 + 1/12CO_2 \rightarrow 1/12CH_4 + 1/6H_2O$, corresponding to $\Delta G' = 0$). The lowest hydrogen partial pressure was derived as 3.476×10^{-6} atm, corresponding to 2.1 nM. By further using equation in Fig. S2, a maximum H_2 flux of approximately 9.8×10^{-9} A can be obtained.

Supplemental Reference:

LIN, R., CHENG, J., DING, L. & MURPHY, J. D. 2018. Improved efficiency of anaerobic digestion through direct interspecies electron transfer at mesophilic and thermophilic temperature ranges.

Chemical Engineering Journal, 350**,** 681-691.

LIN, R., CHENG, J., ZHANG, J., ZHOU, J., CEN, K. & MURPHY, J. D. 2017. Boosting biomethane yield and production rate with graphene: The potential of direct interspecies electron transfer in anaerobic digestion. *Bioresource Technology,* 239**,** 345-352.

STAMS, A. J., DE BOK, F. A., PLUGGE, C. M., VAN EEKERT, M. H., DOLFING, J. & SCHRAA, G. 2006. Exocellular electron transfer in anaerobic microbial communities. *Environmental Microbiology,* 8**,** 371-382.